Heinemann, U., Alings, C., & Lauble, H. (1990), in *Structure & Methods, Volume 3: DNA & DNA* (Sarma, R. H., & Sarma, M. H., Eds.) pp 39–53, Adenine Press, Guilderland, NY.
Horn, T., & Urdea, M. (1986) *Tetrahedron Lett. 27*, 4705.
Kessler, H., Griesinger, C., Zarbock, J., & Loosli, H. R. (1984) *J. Magn. Reson. 57*, 331.
Lilley, D. M. J. (1989) *Chem. Soc. Rev. 18*, 53.
Muller, U. R., & Fitch, W. M. (1982) *Nature (London) 298*, 582.
Puglisi, J. D., & Tinoco, I., Jr. (1989) *Methods Enzymol. 180*, 304.
Senior, M. M., Jones, R. A., & Breslauer, K. J. (1988) *Proc. Natl. Acad. Sci. U.S.A. 85*, 6242.
Shabarova, Z. A. (1988) *Biochemie 70*, 1323.
States, D. J., Haberkorn, R. A., & Ruben, D. J. (1982) *J. Magn. Reson. 48*, 286.
Tebby, J. C. (1987) in *Phosphorus-31 NMR Spectroscopy in Stereochemical Analysis* (Verkade, J. G., & Quin, L. D., Eds.) pp 1–60, VCH, Deerfield Beach, FL.
Wemmer, D. E., & Benight, A. S. (1985) *Nucleic Acids Res. 13*, 8611.
Williams, L. D., & Goldberg, I. H. (1988) *Biochemistry 27*, 3004.
Yager, T. D., & von Hipple, P. H. (1987) in *Cellular and Molecular Biology* (Neidhart, F., et al., Eds.) pp 1241–1275, American Society of Microbiology, Washington, DC.

Kinetic Mechanism of the *Eco*RI DNA Methyltransferase†

Norbert O. Reich* and Neda Mashhoon
Chemistry Department, University of California, Santa Barbara, California 93106
Received July 3, 1990; Revised Manuscript Received December 14, 1990

ABSTRACT: We present a kinetic analysis of the *Eco*RI DNA N^6-adenosine methyltransferase (Mtase). The enzyme catalyzes the *S*-adenosylmethionine (AdoMet)-dependent methylation of a short, synthetic 14 base pair DNA substrate and plasmid pBR322 DNA substrate with k_{cat}/K_m values of 0.51×10^8 and 4.1×10^8 s^{-1} M^{-1}, respectively. The Mtase is thus one of the most efficient biocatalysts known. Our data are consistent with an ordered bi-bi steady-state mechanism in which AdoMet binds first, followed by DNA addition. One of the reaction products, *S*-adenosylhomocysteine (AdoHcy), is an uncompetitive inhibitor with respect to DNA and a competitive inhibitor with respect to AdoMet. Thus, initial DNA binding followed by AdoHcy binding leads to formation of a ternary dead-end complex (Mtase–DNA–AdoHcy). We suggest that the product inhibition patterns and apparent order of substrate binding can be reconciled by a mechanism in which the Mtase binds AdoMet and noncanonical DNA randomly but that recognition of the canonical site requires AdoMet to be bound. Pre-steady-state and isotope partition analyses starting with the binary Mtase–AdoMet complex confirm its catalytic competence. Moreover, the methyl transfer step is at least 10 times faster than catalytic turnover.

The selective recognition and subsequent modification of DNA by enzymes are critical to all known forms of life. A nearly ubiquitous example of such DNA modification is the methylation of cytosine and adenine bases. This expansion of the information content of DNA has biological consequences ranging from protection of host DNA against restriction endonucleases to regulation of gene expression in eukaryotes (Razin et al., 1984; Modrich & Roberts, 1982). Moreover, sequence-specific modification of DNA represents a dramatic achievement in macromolecular recognition. DNA methylation is catalyzed by a diverse group of enzymes which are uniformly dependent on *S*-adenosylmethionine as a methyl donor. Prokaryotic type II DNA Mtases, with hundreds of sequence specificities, form a large subset of DNA-modifying enzymes; their use in molecular biology is widespread (Modrich & Roberts, 1982; Koob et al., 1988). An understanding of the recognition and catalytic mechanisms of these enzymes may facilitate the design of biocatalysts with novel specificities and chemical mechanisms.

We are investigating the *Eco*RI[1] DNA Mtase to understand the details of DNA sequence discrimination, cofactor interactions, and the catalytic mechanism. The *Eco*RI Mtase is functional as a monomer (MW 38050) and is part of a type II bacterial restriction–modification system. The enzyme methylates the second adenine in the canonical site 5′GAATTC3′ to form N^6-methyladenine and *S*-adenosylhomocysteine (AdoHcy), thereby making the site resistant to cleavage by the corresponding *Eco*RI endonuclease (Rubin & Modrich, 1977). The availability of the Mtase gene (Greene et al., 1981), large amounts of highly purified protein, and relatively simple catalytic requirements make this an ideal system to investigate DNA methylation. Moreover, the X-ray structures of the DNA substrate (Drew et al., 1981), methylated DNA product (Frederick et al., 1988), and *Eco*RI endonuclease–DNA complex (McClarin et al., 1986) provide detailed structural information.

One approach to understanding DNA–enzyme interactions is by functional analysis of DNA substrates which lack structural features proposed to be contacted by the enzyme. Interpretation of such detailed specificity analyses is aided by an understanding of the kinetic mechanism; thus, the order

† This work was supported by National Science Foundation Grant DMB 89-11404 to N.O.R.
* To whom correspondence should be addressed.

[1] Abbreviations: *Eco*RI, plasmid-specified DNA restriction–modification system of *Escherichia coli*; DTT, dithiothreitol; EDTA, ethylenediaminetetraacetic acid; AdoMet, *S*-adenosylmethionine; AdoHcy, *S*-adenosylhomocysteine; DE81, diethylaminoethyl ion-exchange filters.

0006-2960/91/0430-2933$02.50/0

of substrate addition, product dissociation, and the assignment of rate-limiting steps are critical. Here we present our results of initial velocity, product inhibition, pre-steady-state, and isotope exchange studies with the *Eco*RI DNA Mtase.

Materials and Methods

[*methyl*-^{3}H]AdoMet (78.9 Ci/mmol) was purchased from New England Nuclear. AdoHcy was purchased from Boehringer Mannheim. Unlabeled AdoMet (chloride salt) and crystalline BSA were purchased from Sigma. Dithiothreitol and *Pvu*II endonuclease were from Bethesda Research Laboratories. Glycerol (enzyme grade) was from Fisher Scientific. DE81 anion-exchange filter papers were from Whatman. Liquiscint scintillation fluid was from National Diagnostics.

*Eco*RI DNA Mtase was purified from *Escherichia coli* strain MM294 harboring plasmid pPG440 (Greene et al., 1978). The concentration of *Eco*RI Mtase was determined spectrophotometrically [$E^{1\%}$ at 278 nm = 10.8 (Rubin & Modrich, 1977)]. Synthetic oligonucleotides (5′GGCGGAATTCGCGG3′, 5′CCGCGAATTCCGCC3′, 5′GGCGAmATTCGCGG3′, and 5′CCGCGAmATTCCGCC3′; mA = N^6-methyladenosine) were prepared on a BioSearch 3810 DNA synthesizer using β-cyanoethyl phosphoramidites. Oligonucleotides were purified on a C_{18} reverse-phase HPLC column (Becker et al., 1983). Oligonucleotide composition was determined by HPLC analysis of the corresponding nucleotides generated by digestion with phosphodiesterase and alkaline phosphatase. Oligonucleotide purity was confirmed by ^{32}P radiolabeling and subsequent autoradiography using DNA sequencing gels. The concentrations of single strands were determined spectrophotometrically. Confirmation of the double-stranded form was through autoradiography with nondenaturing polyacrylamide gel electrophoresis. The thermal stabilities of the double-stranded DNA [14-mer, top strand = 5′GGCGGAATTCGCGG3′; methylated 14-mer (m14-mer), top strand = 5′GGCGGAmATTCGCGG3′, bottom strand = 5′CCGCGAmATTCCGCC3′] were determined spectrophotometrically. Plasmid pBR322 was isolated from *E. coli* strain MM294 by alkaline lysis (Maniatis et al., 1982) and further purified by size-exclusion chromatography and C_{18} reverse-phase HPLC (Colote et al., 1986). Purified plasmid pBR322 was linearized by hydrolysis with *Pvu*II endonuclease to yield a molecule with a unique *Eco*RI site positioned 2295 nucleotides from the 5′ end and 2068 nucleotides from the 3′ end. After heat inactivation of the endonuclease, the linearized DNA was dialyzed against 10 mM Tris, pH 7.5, and 1 mM EDTA for 15 h and stored at −20 °C. The concentration of plasmid DNA was determined spectrophotometrically. Unlabeled AdoMet purchased from Sigma was approximately 87% pure; this was further purified by using an HRLC MA7S (50 × 7.8 mm) cation-exchange column according to a modified procedure of Zappia et al. (1980). Ammonium acetate buffer (0.1 M, pH 4.0) was used to elute AdoMet at a flow rate of 1 mL/min. The peak corresponding to AdoMet was collected, concentrated on a BioRex 70 cation-exchange column (Bio-Rad), and stored at −20 °C in 0.1 N HCl (Reich & Everett, 1990).

Mtase Assay. All Mtase assays monitored the incorporation of tritiated methyl groups into DNA by using an ion-exchange filter assay (Rubin & Modrich, 1977). Reactions contained 100 mM Tris, pH 8.0, 10 mM EDTA, 200 μg/mL BSA, and 10 mM DTT (MR buffer). Substrate concentrations (DNA and AdoMet) were as noted in each experiment. [*methyl*-^{3}H]AdoMet was 13 000–70 000 cpm/pmol. The Mtase was diluted in protein dilution (PD) buffer: 20 mM potassium phosphate, pH 7.4, 200 mM NaCl, 0.2 mM EDTA, 200 μg/mL BSA, 2 mM DTT, and 10% (v/v) glycerol. After incubation at 37 °C, samples were stopped by transferring aliquots to 2 × 2 cm squares of Whatman DE81 filter papers. Filters were washed 3 times (10 min each) with 50 mM KH_2PO_4, once with 80% ethanol, once with 95% ethanol, and once with diethyl ether. Filters were air-dried, and tritium content was determined in 4 mL of Liquiscint using a Beckman Model LS 1701 scintillation counter.

Initial Velocity Studies. To a 50-μL reaction volume containing *Eco*RI Mtase (0.2 nM unless otherwise indicated) were added all but the varied component described in each figure. The reaction was initiated upon addition of the varied component. Reactions were stopped by placing 40 μL of the reaction onto DE81 filter paper and processed as described above. When indicated, the products (methylated 14-mer and AdoHcy) were added in the preincubation period prior to addition of varied substrate.

Pre-Steady-State Studies. A 20-μL reaction volume containing MR buffer, Mtase (3 μM, unless otherwise indicated), and radiolabeled AdoMet (30 μM) was preincubated at 37 °C for 3 min. A 4-μL aliquot was removed and brought to a final volume of 200 μL containing MR buffer, 30 μM labeled AdoMet, and various concentrations of DNA (14-mer) at 37 °C. Aliquots (30 μL) of this "chase" reaction were analyzed as described above at the indicated times.

Isotope Partition Studies. These protocols were identical with those described for the pre-steady-state experiments with the following changes: (1) the AdoMet (30 μM) in the chase was not radiolabeled; or (2) 4 μL of the preincubation was combined with all chase components (including unlabeled AdoMet) except DNA, which was added after the 3-min preincubation at 37 °C.

Data Analysis. Unless otherwise indicated, all enzyme activity data are the average of at least duplicate determinations. All kinetic data were analyzed by using a BASIC version of the Cleland (1979) programs. Initial velocity results were analyzed with eq 1 (SEQUEN program) and a modified version of eq 1 in which the K_{ia} term was replaced by the K_d for AdoMet (30 μM).

$$v = V_m AB/(K_{ia}K_b + K_bA + K_aB + AB) \quad (1)$$

Data from product inhibition experiments were fitted to linear competitive (COMP), noncompetitive (NONCOMP), and uncompetitive (UNCOMP) models (eq 2–4, respectively),

$$v = V_m A/[K_a(1 + I/K_{is}) + A] \quad (2)$$

$$v = V_m A/[K_a(1 + I/K_{is}) + A(1 + I/K_{ii})] \quad (3)$$

$$v = V_m A/[K_a + A(1 + I/K_{ii})] \quad (4)$$

and K_i values for each product were obtained. The suggested statistical criteria of Cleland (1979) were used to determine which model provided the best fit to the data. Standard errors are shown with all data as calculated by the Cleland programs (Cleland, 1979).

Results

Preliminary Characterization of Substrates and Reaction Conditions. The design of the non-self-complementary 14 base pair oligonucleotide substrate (14-mer) was based on two concerns. First, it was imperative that the DNA substrate remain double stranded under the salt and DNA concentrations, as well as the temperature conditions of the enzyme assays. On the basis of spectrophotometrically derived melting temperatures the 14-mer and methylated 14-mer are greater

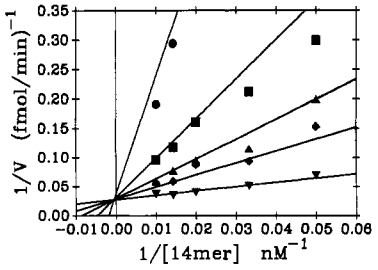

FIGURE 1: Steady-state kinetics of *Eco*RI DNA Mtase with 14-mer DNA substrate. Reactions contained 14-mer (20–100 nM) and [*methyl*-^{3}H]AdoMet, 0.05 (●), 0.1 (■), 0.3 (▲), 1.0 (♦), and 3.0 (▼) μM, in MR buffer. *Eco*RI Mtase was diluted in PDB to a final concentration of 0.1 nM. Incubations were for 16 min at 37 °C.

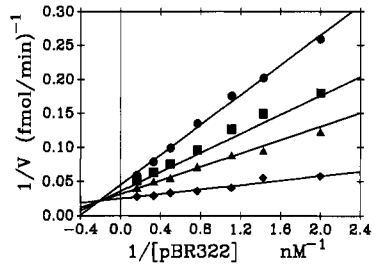

FIGURE 2: Steady-state kinetics of *Eco*RI DNA Mtase with linearized plasmid pBR322. Reactions contained DNA (0.5–6.0 nM) and [*methyl*-^{3}H]AdoMet, 0.2 (●), 0.4 (■), 0.6 (▲), and 3.0 (♦) μM, in MR buffer. *Eco*RI Mtase was diluted in PDB to a final concentration of 0.1 nM. Incubations were for 5 min at 37 °C.

than 90% double stranded under our assay conditions (Danzitz and Reich, unpublished results). Moreover, the presence of excess single strands was shown not to interfere with enzyme activity (Danzitz and Reich, unpublished results). Second, our DNA footprinting studies showed that the Mtase interacts with two bases beyond the recognition hexanucleotide (Reich and Danzitz, unpublished results). A minimum length of 10 bases is therefore required.

The pH optimum for enzymic activity, determined at single concentrations of DNA (14-mer) and AdoMet, is 7.8. The optimal activity at pH 8.0 occurs between 10 and 20 mM NaCl. For all conditions of DNA and AdoMet concentrations used in this report, the rate of methylated DNA formation was shown to be constant with respect to time. Enzyme activity under steady-state conditions was linear from 0.1 to 30 nM Mtase. No product inhibition was indicated under the initial velocity conditions; the derived binding constants for methylated DNA and AdoHcy (see below) are consistent with this observation. All substrate DNA concentrations refer to *Eco*RI sites.

Velocity Dependence on DNA and AdoMet Concentrations. Initial velocity data were determined at various concentrations of [*methyl*-^{3}H]AdoMet and DNA (14-mer or plasmid pBR322). We have included linearized plasmid DNA to determine if Mtase interactions with the larger, more biologically relevant substrate are kinetically similar to those found with small substrates. The double-reciprocal plot of 1/velocity ($1/V$) versus 1/DNA concentration (14-mer, Figure 1) using eq 1 gave a series of lines intersecting close to but not on the $1/V$ axis, thus suggesting that a ping-pong mechanism is unlikely. Equation 1 (with K_{ia}^{AdoMet} set at 30 μM) gave the best fit to our data. The data for plasmid pBR322 (Figure 2) were best fit with eq 1, without using a predefined value for K_{ia}^{AdoMet}. A plausible explanation for this distinction is presented in the context of our proposed kinetic mechanism (see Discussion). All data were fit to PINGPONG, EQORD, and SEQUEN programs (Cleland, 1979); comparison of standard

Table I: Kinetic Parameters Obtained with the 14-mer and pBR322 DNA Substrates[a]

	14-mer	plasmid pBR322	source of data
k_{cat} (s^{-1})	0.124 (0.006)	0.142 (0.006)	Figures 1 and 2
K_m^{DNA} (nM)	2.44 (0.31)	0.346 (0.092)	Figures 1 and 2
K_m^{AdoMet} (nM)	118 (125)	210 (50)	Figures 1 and 2
k_{cat}/K_m^{DNA} (s^{-1} M^{-1})	0.51×10^8	4.1×10^8	Figures 1 and 2
K_d^{DNA} (nM)		>1000–4000	*b*
K_d^{AdoMet} (μM)	30		*c*
K_d^{AdoHcy} (μM)	220–250		*d*

[a] Values in parenthese are the standard error. Data analysis was as described under Materials and Methods. [b] The DNA used in this assay was a 146 bp restriction fragment isolated from plasmid pBR322 which contains one canonical *Eco*RI site, and K_d^{DNA} represents a lower limit (Reich & Mashhoon, 1990). [c] K_d^{AdoMet} was determined with a pre-steady-state analysis (data not shown) (Materials and Methods). [d] The dissociation constant for AdoHcy was determined by using a competitive pre-steady-state analysis (Reich & Mashhoon, 1990) and inhibition of in vitro proteolysis of the Mtase (Reich et al., 1991).

deviations demonstrated the data best fit the SEQUEN program, consistent with either ordered steady-state or random rapid equilibrium mechanisms. Although not shown, intercept and slope replots of all double-reciprocal data are linear, suggesting that a steady-state random mechanism is not valid.

The double-reciprocal analyses shown in Figures 1 and 2 for the 14-mer and plasmid pBR322 were used to obtain the catalytic turnover constant (k_{cat}), Michaelis constants for AdoMet (K_m^{AdoMet}) and DNA (K_m^{DNA}), and the specificity constant (k_{cat}/K_m) for DNA shown in Table I. The k_{cat} for the *Eco*RI DNA Mtase is significantly higher than that measured for other DNA Mtases: 2.1×10^{-4} s^{-1} for *Eco*P15 (Rao et al., 1989), 0.067 s^{-1} for *Bam*HI (Nardone et al., 1986), and 0.022 s^{-1} for *Hha*I (Wu & Santi, 1987). The similarity of the methylation rate constants for the short (14-mer) and long (4363 bp) DNA substrates is consistent with the *Eco*RI DNA Mtase having similar rate-limiting step(s) with both substrates. In contrast, the Michaelis constant (defined as canonical site concentration) for plasmid pBR322 is 7-fold smaller than that determined for the 14-mer. This saturation at lower site concentration does not derive simply from differences in the immediate flanking sequence; DNA substrates with different flanking sequences have K_m values similar to those found for the 14-mer (Reich & Mashhoon, 1990). Comparison of $k_{cat}/K_m^{14\text{-mer}}$ and k_{cat}/K_m^{pBR322} shows that the Mtase catalyzes methylation of plasmid pBR322 at least 8-fold more efficiently than the synthetic 14-mer.

Product Inhibition Studies. We performed a variety of product inhibition analyses to further distinguish between ordered and random mechanisms. These data are summarized in Table II. Slope replots for the competitive inhibition observed with AdoMet and AdoHcy (for both the 14mer and plasmid pBR322) are linear, consistent with simple competitive inhibition (data not shown). The competitive inhibition shows that in the presence of either DNA substrate, AdoMet and AdoHcy compete for the same form of the enzyme. The inhibition constants (Table II) are significantly lower than the dissociation constant for the Mtase–AdoHcy complex determined by competitive pre-steady-state methods and in vitro proteolysis (Table I). The enhanced affinity of the enzyme for AdoHcy in the presence of DNA most likely derives from the formation of a ternary complex (Mtase–DNA–AdoHcy).

Further support for such a complex is provided by the uncompetitive inhibition observed for AdoHcy and DNA (Figures 3 and 4). Application of the statistical criteria of Cleland (1979) to these data as well as on duplicate sets of experiments suggests that the patterns are uncompetitive. The uncom-

Table II: Product Inhibition of *Eco*RI DNA Mtase[a]

product	variable substrate	fixed substrate	type of inhibition	inhibition constant
DNA^m*	DNA	AdoMet	NC[d]	67.3 nM (17.3)
DNA^m*	AdoMet	DNA(14-mer)	NC[e]	31.9 nM (7.4)
AdoHcy	AdoMet	DNA(14-mer)	C[f]	9.3 μM (0.9)
AdoHcy	DNA (14-mer)	AdoMet	UC	8.5 μM (0.9)[b]
AdoHcy	AdoMet	DNA(plasmid)	C[g]	28.1 μM (3.1)
AdoHcy	DNA (plasmid)	AdoMet	UC	112.9 μM (18.3)[c]

[a] Values in parentheses are the standard error. NC, noncompetitive; C, competitive; UC, uncompetitive; asterisk, using methylated 14-mer. [b] Data obtained shown in Figure 3. [c] Data shown in Figure 4. [d] Assay conditions as described under Materials and Methods using 14-mer (15–100 nM), 0.4 μM AdoMet, 0.2 nM Mtase, and methylated 14-mer (0, 30, 60, 125, and 250 nM). [e] Assay conditions included AdoMet (0.2–3.0 μM), 14-mer (35 nM), methylated 14-mer (0, 30, 60, 250, and 500 nM), and 0.4 nM Mtase. [f] Assay conditions included AdoMet (0.1–1.0 μM), 14-mer (100 nM), AdoHcy (0, 10, 30, and 50 μM), and 0.2 nM Mtase. [g] Assay conditions included AdoMet (0.06–1.0 μM), linearized pBR322 (6.0 nM), AdoHcy (0, 10, 30, 50, and 100 nM), and 0.1 nM Mtase.

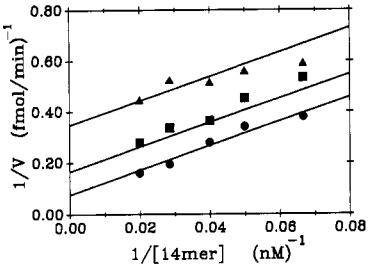

FIGURE 3: Product inhibition by AdoHcy versus 14-mer. Reciprocal plot of methylation rate versus 14-mer concentration (15–50 nM) in the presence of subsaturating [*methyl*-^{3}H]AdoMet concentration (0.2 μM). AdoHcy concentrations were 0 (●), 10 (■), and 30 (▲) μM. Reactions contained 0.1 nM Mtase. Incubations were for 12 min at 37 °C.

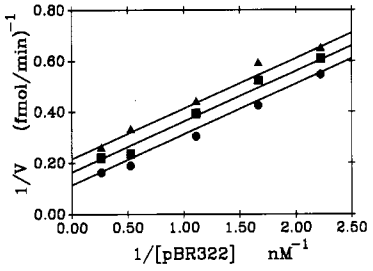

FIGURE 4: Product inhibition by AdoHcy versus linearized plasmid pBR322. Reciprocal plot of methylation rate versus pBR322 concentration (0.45–3.8 nM) in the presence of subsaturating [*methyl*-^{3}H]AdoMet concentration (0.15 μM). AdoHcy concentrations were 0 (●), 50 (■) and 100 (▲) μM. Reactions contained 0.1 nM Mtase, and incubations were for 20 min at 37 °C.

petitive pattern is consistent with a mechanism in which AdoHcy binds to a Mtase–DNA complex, forming a catalytically incompetent ternary complex.

To further distinguish between ordered and random mechanisms and to characterize the order of substrate binding, we determined the inhibition pattern with methylated DNA and DNA at saturating AdoMet concentrations (Table II). The observed noncompetitive pattern is inconsistent with any ordered mechanism in which DNA is required to bind first. Consistent with the observed pattern are an AdoMet first, ordered steady-state mechanism.

The mixed-type pattern observed with AdoMet and methylated DNA (Table II) is consistent with an AdoMet first, ordered steady-state mechanism, but not the corresponding

Scheme I: Proposed Kinetic Mechanism for the *Eco*R1 DNA Mtase[a]

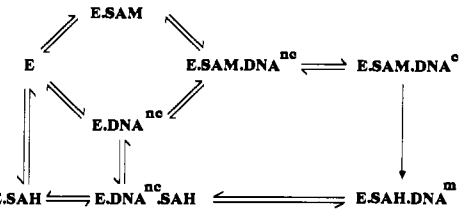

[a] DNA^{nc}, DNA^c, and DNA^m represent noncanonical, canonical, and methylated DNA, respectively. SAM, AdoMet; SAH, AdoHcy.

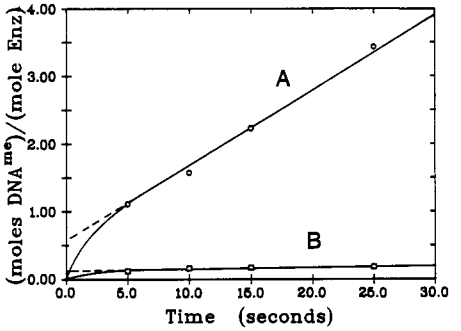

FIGURE 5: Pre-steady-state kinetics of the *Eco*RI DNA Mtase starting with the Mtase–AdoMet complex. Moles of methylated DNA were determined (see Materials and Methods) after a 4-μL preincubation of Mtase (3 μM), and labeled AdoMet (30 μM) was diluted 50-fold into (A) labeled AdoMet (30 μM) and DNA (14-mer, 200 nM) or (B) unlabeled AdoMet (30 μM) and DNA (14-mer, 200 nM).

rapid equilibrium mechanism.

The combined double-reciprocal and product inhibition analyses along with the catalytic competence of the Mtase–AdoMet complex (see below) suggest an ordered steady-state mechanism in which the enzyme binds first to AdoMet. The uncompetitive inhibition plots (Figures 3 and 4) suggest AdoHyc binds to the Mtase–DNA complex. To reconcile this latter binding order with the proposed order of substrate binding, we propose a kinetic scheme in which the enzyme binds randomly to flanking, or noncanonical DNA (DNA^{nc}) and AdoMet to form a Mtase–DNA^{nc}–AdoMet complex. This ternary complex is then converted to Mtase–DNA^c–AdoMet (canonical DNA, DNA^c). The apparent order derives from the requirement for AdoMet to be bound prior to the conversion. Scheme I describes this mechanism.

Pre-Steady-State and Isotope Partitioning Studies. We used pre-steady-state kinetic analysis to elucidate which steps limit catalytic turnover. Preincubation of high (micromolar) *Eco*RI Mtase concentrations with 30 μM radiolabeled AdoMet results in a "burst" of product (methylated 14-mer) formation upon addition of DNA (14-mer) and labeled AdoMet, shown in Figure 5, line A. The burst is followed by a constant rate of product formation [0.15 pmol of product (pmol of enzyme)$^{-1}$ s^{-1}], similar to the catalytic turnover constant measured under steady-state conditions (Table I). Thus, starting from the Mtase–AdoMet complex, the rate constant for product formation is significantly larger during the first few seconds than the catalytic rate constant. The simplest interpretation of these data is that DNA methylation is followed by a slower step (or steps) and this slower step is detected as the catalytic rate constant.

We determined that the burst magnitude was dependent on the AdoMet and Mtase concentrations in the preincubation as well as the DNA concentration in the chase (data not shown). (We define burst magnitude in our analysis as the vertical axis intercept resulting from extrapolation of the linear portion of the progress curve to zero time.) For example, 70

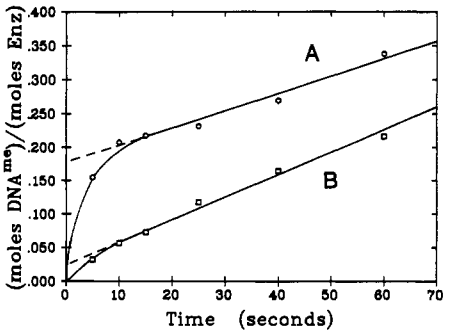

FIGURE 6: Isotope partitioning analysis of the *Eco*RI DNA Mtase starting with the Mtase–AdoMet complex. Line A is the identical data shown in Figure 5 (line B). The data for line B were obtained as for line A except that the preincubation of Mtase and labeled AdoMet was first combined with unlabeled AdoMet (50-fold molar excess of unlabeled over labeled) and then followed by addition of DNA (14-mer, 200 nM).

nM DNA resulted in half-maximal burst size, and hence all pre-steady-state and isotope partitioning experiments were done with 200 nM DNA in the chase. The corresponding experiments in which the AdoMet concentration was varied in the preincubation at constant DNA concentration (200 nM) in the chase showed that the amount of AdoMet required to attain half-maximal burst size was 30 μM. The burst magnitudes in these latter experiments were used to approximate the moles of enzyme bound to AdoMet in the preincubation (Rose, 1980) and, subsequently, the dissociation constant for the Mtase–AdoMet binary complex (Table I). The 30 μM dissociation constant is consistent with our determinations using equilibrium dialysis (Reich & Everett, 1990) and in vitro proteolysis (Reich et al., 1991).

As a result of low radioactivity incorporation due to the specific activity of radiolabeled AdoMet, we used 30 μM AdoMet in all pre-steady-state and isotope partition experiments. On the basis of the 30 μM dissociation constant for the binary complex, only 50% of the enzyme is expected to be bound under these conditions. In Figure 5, line A, the vertical axis intercept corresponds to 0.6 mol of DNA methylated per mole of Mtase in the preincubation; thus, 60% of the Mtase was bound to AdoMet in the preincubation. The similarity of this value to the predicted level of binary complex confirms that the entire Mtase sample is active (Fersht, 1985). The burst magnitude would be equivalent to the concentration of the Mtase–AdoMet complex if DNA concentrations were in excess of K_m and the methylation rate constant (k_{meth}) were much greater than rate constants for subsequent steps (k_f) (Hiromi, 1979). This relationship is shown in eq 5, in which the burst magnitude (BM) and the quantity of enzyme (Mtase–AdoMet complex, E^0) are given in moles. Since the

$$(BM)^{-1/2} = (E^0)^{-1/2}(1 + k_f/k_{meth})(1 + K_m^{DNA}/[DNA]) \quad (5)$$

DNA concentration in the chase is 200 nM and the K_m^{DNA} is 2.44 nM, the right side of eq 5 reduces to a product of the enzyme amount and the relative rate constant term ($1 + k_f/k_{meth}$). If k_{meth} is 20 times k_f, then the burst magnitude is 90% of E^0; if k_{meth} is 5 times k_f, then the value drops to 80%. On the basis of the data shown in Figure 5, we estimate that k_{meth} is at least 10 times k_f.

We used the isotope exchange method described by Rose (1980) to confirm the catalytic competence of the Mtase–AdoMet complex. Our experiments shown in Figure 5 (line B) and Figure 6 (lines A and B) were also undertaken to determine the extent to which the Mtase–AdoMet complex partitions between product formation (DNA addition) and AdoMet release. Both of these issues are relevant to the kinetic mechanism since Scheme I requires that the binary Mtase–AdoMet complex is capable of forming the ternary complex leading to catalysis. Line B (Figure 5) shows a decreased burst size as a result of substituting unlabeled AdoMet (plus DNA) in the chase. This burst, although 3.5-fold smaller than in line A (Figure 5), is real since coincubation of the labeled and unlabeled AdoMet with Mtase prior to DNA addition shows a much smaller burst (line B, Figure 6). These data provide direct evidence that the Mtase–AdoMet complex is kinetically competent and preclude any kinetic mechanism which requires DNA to be bound first. Moreover, the size of the burst with the unlabeled chase requires that the dissociation rate constant from the Mtase–AdoMet complex be comparable to the rate constant for the first irreversible step (presumably methylation).

Discussion

Our goal was to elucidate the kinetic mechanism of *Eco*RI DNA Mtase with a small synthetic DNA substrate and a plasmid substrate containing a single canonical site.

Steady-State Kinetic Parameters. The steady-state kinetic parameters in Table I reveal subtle differences in Mtase interactions with the two DNA substrates. The first indication of a difference came in applying eq 1 to fit our double-reciprocal data. Although the 14-mer data fit the equation well when K_{ia}^{AdoMet} was set to 30 μM (Table I), the plasmid data required no preset value for K_{ia}^{AdoMet}. A plausible explanation based on our proposed mechanism (Scheme I) is that ternary complexes (Mtase–DNA^{nc}–AdoMet) at noncanonical sites may occur. The fraction of the Mtase in these complexes could contribute to the K_{ia}^{AdoMet} term, and since the magnitude of this effect is expected to depend on the noncanonical site concentration, this effect is predicted to be more significant with the large plasmid substrate. In other words, setting K_{ia}^{AdoMet} equal to K_d^{AdoMet} is acceptable for the 14-mer with few noncanonical sites, but the large DNA substrate provides so many noncanonical sites that the "real" K_{ia}^{AdoMet} is much lower. The best fit for the large DNA is thus obtained only if the K_{ia}^{AdoMet} is not set. Second, the K_m^{DNA} is over 7 times lower for plasmid DNA than the synthetic oligonucleotide; similar results were obtained for *Eco*RI endonuclease (Greene et al., 1975). An explanation for these K_m^{DNA} differences with the endonuclease is that the decreased K_m^{DNA} results from increased rates of association (k_{on}) (Jack et al., 1982). Implicit in this explanation is that the endonuclease and presumably the Mtase locate their canonical sites by processive movement along the DNA, a result confirmed with the endonuclease (Jack et al., 1982) and by our preliminary results with the Mtase.[2]

The similarity in turnover constants (k_{cat}) for the 14-mer and plasmid DNA substrates suggests the Mtase has similar rate-limiting steps with both substrates. Since our pre-steady-state data with the 14-mer show that the rate-limiting steps occur after methylation, it is likely that similar product release steps limit catalytic turnover. The differences in specificity constants (k_{cat}/K_m^{DNA}) are thus due to the differences in K_m^{DNA} and as suggested earlier may derive from changes in association kinetics. Comparison of k_{cat}/K_m for other efficient enzymes shows the *Eco*RI Mtase to be one of the most efficient enzymes reported, suggesting that a physical associative process is limiting the second-order specificity

[2] N. O. Reich and M. Surby, unpublished results.

constant (Fersht, 1985). However, comparisons of the Mtase with other enzymes at this level are inherently misleading; different constraints on k_{cat}/K_m may apply for enzymes interacting with polymeric substrates like DNA. This is suggested by studies with the *lac* repressor, which showed that the association rate constant for the protein with its operator DNA on large DNA molecules ranges up to 5×10^{10} s^{-1} M^{-1} (Riggs et al., 1970). This association rate constant is over 500 times faster than the predicted limit determined for diffusion through solution and has been explained by a processive translocation mechanism (Riggs et al., 1970; von Hippel & Berg, 1989; Barkeley, 1981; Jack et al., 1982; Singer & Wu, 1987). Thus, based on analogy with the *lac* repressor, the Mtase specificity constant, although extremely high when compared to other enzymes, could theoretically be at least 100-fold higher.

Finally, although extrapolation of our in vitro data to events occurring within the bacterial cell may be simplistic, comparison of our data with the Mtase and similar specificity data for the *Eco*RI endonuclease suggests that bacterial host viability may derive at least in part from the Mtase being over 45-fold more efficient than the endonuclease (Hager et al., 1990).

Kinetic Mechanism. Our assignment of the kinetic mechanism rests on three lines of evidence. First, a steady-state mechanism is supported by the large specificity constants discussed in the previous paragraphs (Fersht, 1985). Second, the patterns of lines in initial velocity (Figures 1 and 2) and product inhibition studies (Figures 3 and 4, Table II) are shown to be inconsistent with random mechanisms as well as mechanisms in which DNA binding is required to occur first. Third, pre-steady-state and isotope partition experiments (Figures 5 and 6) are used to show that steps after methylation determine k_{cat}, and to confirm the catalytic competence of the Mtase–AdoMet complex. We propose a kinetic mechanism (Scheme I) which is consistent with all of our data, for both the 14-mer and plasmid substrates.

A ping-pong mechanism is unlikely since the patterns in Figures 1 and 2 are intersecting and some form of ternary complex (Mtase–DNA–AdoMet) is therefore indicated. The simple competitive plots for AdoMet and AdoHcy at constant DNA concentrations (Table II) rule out a steady-state mechanism in which DNA and AdoMet bind randomly (Segel, 1975).[3]

The uncompetitive inhibition observed with AdoHcy and DNA at a constant AdoMet concentration (Figures 3 and 4) also argues against random mechanisms; this pattern and the differences between the inhibition constants (K_i^{AdoHcy}) and dissociation constants (K_d^{AdoHcy}) suggest that a binary Mtase–DNA complex can bind AdoHcy. Although several mechanisms might include such a dead-end complex, the predicted patterns for most such mechanisms are not uncompetitive. For example, a dead-end Mtase–DNA–AdoHcy complex with a random, rapid equilibrium mechanism, requires a mixed-type, not an uncompetitive plot. Uncompetitive plots are also not predicted for a random steady-state mechanism. Thus, a steady-state ordered mechanism is suggested.

Additional evidence against a random rapid equilibrium mechanism and a DNA first-ordered mechanism is provided by the noncompetitive inhibition pattern observed with methylated 14-mer and 14-mer (Table II), since a competitive plot is expected in these cases (Segel, 1975). Although consistent with both an ordered AdoMet first (rapid equilibrium binding) and random steady-state mechanisms (Segel, 1975), such mechanisms are inconsistent with much of our other data. For example, to generate a noncompetitive pattern, the latter mechanism requires the formation of an inhibitory Mtase–DNA–DNA^m complex, which is unlikely on two grounds: (1) On the basis of analysis of structurally characterized protein–DNA complexes, a Mtase–DNA–DNA^m complex seems unlikely with a monomeric 38-kDa protein. (2) An inhibitory Mtase–DNA–DNA complex would reasonably be expected to form as well, resulting in substrate inhibition which was not observed in these analyses.

The reconciliation of the uncompetitive patterns (Figures 4 and 5), competitive, and noncompetitive patterns (Table II) with the pre-steady-state analysis (Figures 5 and 6) forms the basis of the kinetic mechanism assignment described earlier, and elaborated below. We propose that the Mtase has a steady-state ordered mechanism in which the free enzyme binds to AdoMet first, followed by DNA binding. After methyl transfer, the DNA^m is released, followed by AdoHcy release. Support for this model comes from the double-reciprocal analysis (Figure 1) and the competitive inhibition seen between AdoMet and AdoHcy (Table II). The uncompetitive inhibition observed in Figure 3 requires that AdoHcy binds to the binary Mtase–DNA complex, and thus a pathway leading to formation of the dead-end ternary complex, Mtase–DNA–AdoHcy, is included. Finally, the noncompetitive patterns observed for DNA and DNA^m, and AdoMet and DNA^m (Table II) are also consistent with the ordered mechanism. Scheme I incorporates this mechanism along with two additional observations. First, if AdoHcy can bind to the binary Mtase–DNA complex (as supported by Figures 3 and 4), then AdoMet would reasonably be expected to do so also. Second, the polymeric nature of DNA allows for enzyme binding to flanking DNA (DNA^{nc}) to be kinetically distinguishable from binding to the canonical site. Thus, Mtase binding to AdoMet or DNA^{nc} to form the ternary Mtase–DNA^{nc}–AdoMet complex may be random; however, only the AdoMet-bound form of the enzyme recognizes the canonical site. The apparent order (AdoMet binding first) comes from the requirement for AdoMet binding for canonical site recognition (conversion of the Mtase–DNA^{nc}–AdoMet to the Mtase–DNA^c–AdoMet complex).

Assignment of Rate-Limiting Steps and Competency of Mtase–AdoMet Complex. On the basis of the concept of evolutionary perfection of enzyme function (Burbaum et al., 1989), k_{cat} for the highly efficient *Eco*RI Mtase should not be limited by chemical transformation steps (e.g., methyl transfer from AdoMet to DNA). Our pre-steady-state experiments starting with the Mtase–AdoMet complex confirm this prediction (Figures 5 and 6). The rate constant for methylation is at least 10 times larger than subsequent steps which determine k_{cat}. Steps contributing to k_{cat} may be grouped as "product release" processes: movement to flanking (DNA^{nc}) sites, DNA^m release, release of AdoHcy, or any conformational changes required for these events. If the Mtase leaves a methylated site by way of flanking DNA, then the similarity of k_{cat} for DNA substrates of such different lengths (14-mer and pBR322) suggests that Mtase dissociation from DNA is not rate limiting. Alternatively, for AdoHcy release to contribute to k_{cat}, the association rate constant for free Mtase and AdoHcy binding would have to be less than 1000 s^{-1} M^{-1}

[3] Alternatively, a random mechanism might generate this competitive plot if one portion of a random pathway were isolated as a result of using high DNA concentrations. Since the DNA concentrations ranged from 6 to 100 nM [well below the K_d^{DNA} of 1–4 μM estimated as a lower limit (Reich & Mashhoon, 1990)], no isolation of one portion of a random mechanism is predicted.

[given the dissociation constant for the binary Mtase–AdoHcy complex, K_d^{AdoHcy} (Table I)]. Although theoretically possible, such a slow association rate seems highly unlikely (Fersht, 1985). The steps which most likely contribute to k_{cat} thus involve conversion of the ternary complex (Mtase–DNA^m–AdoHcy) to an intermediate in which the enzyme is reassociated with flanking DNA (Mtase–DNA^{nc}–AdoHcy).

The isotope exchange experiments (Figures 5 and 6) provide direct evidence for the competency of the Mtase–AdoMet complex.[4] This is shown by "chasing" the labeled Mtase–AdoMet complex with unlabeled AdoMet and DNA (Figure 5, line B; Figure 6, line A) and observing a reduced, but real, burst. If binding DNA first were required, then the required release of labeled AdoMet would have reduced the burst size to the level of that shown for line B, Figure 6. The magnitude of the burst under these conditions also shows that rate constants for the release of AdoMet from the Mtase–AdoMet complex and for continuing on toward catalysis (e.g., DNA binding and methyl transfer) are similar. This provides further evidence that this portion of the kinetic mechanism is close to a steady-state rather than rapid equilibrium condition.

Conclusions

The proposed mechanism is an apparent ordered steady-state mechanism in which AdoMet binds first. A comprehensive model taking into account an uncompetitive inhibition pattern between DNA and AdoHcy as well as the polymeric nature of the DNA substrates allows for random binding of DNA^{nc} and AdoMet, with recognition of DNA^c requiring AdoMet binding (Scheme I). Our study of the *Eco*RI DNA Mtase shows that kinetic analyses of enzymes interacting with polymeric substrates (e.g., DNA) require alternative solutions. One example of this is the distinction between protein binding to flanking (noncanonical) DNA and canonical site binding; in terms of "substrate binding", these steps are distinct. Another is the upper limit set on k_{cat}/K_m by diffusional constraints; enzymes modifying specific sites in DNA should theoretically be able to attain k_{cat}/K_m values of 5×10^{10} s^{-1} M^{-1} or higher.

Acknowledgments

We thank Mr. Michael J. Danzitz, Jr., for preparing the synthetic oligonucleotides and Dr. William Jack and Dr. Vernon Anderson for helpful discussions.

References

Barkley, M. D. (1981) *Biochemistry 20*, 3833–3842.
Becker, C. R., Efcavitch, J. W., Heiner, C. R., & Kaiser, N. F. (1985) *J. Chromatogr. 326*, 293–299.
Burbaum, J. J., Raines, R. T., Albery, W. J., & Knowles, J. R. (1989) *Biochemistry 28*, 9293–9305.
Cleland, W. W. (1979) *Methods Enzymol. 63*, 103.
Colote, S., Ferraz, C., & Liautard, J. P. (1986) *Anal. Biochem. 154*, 15–20.
Drew, H. R., Wing, R. M., Takano, T., Broka, C., Tanaka, S., Itakura, K., & Dickerson, R. E. (1981) *Proc. Natl. Acad. Sci. U.S.A. 78*, 2179–2183.
Fersht, A. (1985) in *Enzyme Structure and Mechanism*, W. H. Freeman and Co., New York.
Frederick, C. A., Quigley, G. J., van der Marel, G. A., van Boom, J. H., Wang, A. H.-J., & Rich, A. (1988) *J. Biol. Chem. 263*, 17872–17879.
Greene, P. J., Heynecker, H. L., Bolivar, F., Rodriquez, R. L., Betlach, M. C., Covarrubias, A. A., Bachman, K., Russel, D. J., Tait, R., & Boyer, H. W. (1978) *Nucleic Acids Res. 5*, 2373–2380.
Greene, P. J., Gupta, M., Boyer, H. W., Brown, W. E., & Rosenberg, J. M. (1981) *J. Biol. Chem. 256*, 2143–2153.
Hager, P. W., Reich, N. O., Day, J. P., Boyer, H. W., Rosenberg, J. M., & Greene, P. J. (1990) *J. Biol. Chem.* (in press).
Hiromi, K. (1979) in *Kinetics of Fast Enzyme Reactions: Theory and Practice*, John Wiley and Sons, New York.
Jack, W. E., Terry, B. J., & Modrich, P. (1982) *Proc. Natl. Acad. Sci. U.S.A. 79*, 4010–4014.
Koob, M., Grimes, E., & Szybalski, W. (1988) *Science 241*, 1084–1086.
Maniatis, T., Fritsch, E. F., & Sambrook, J. (1982) in *Molecular Cloning*, Cold Spring Harbor Laboratory, Cold Spring Harbor, NY.
McClarin, J. A., Frederick, C. A., Wang, B.-C., Greene, P., Boyer, H. W., Grable, J., & Rosenberg, J. M. (1986) *Science 234*, 1526–1541.
Modrich, P., & Roberts, R. J. (1982) in *Nucleases* (Linn, S. M., & Roberts, R. J., Eds.) Cold Spring Harbor Laboratory, Cold Spring Harbor, NY.
Nardone, G., George, J., & Chirikjian, J. G. (1986) *J. Biol. Chem. 261*, 12128–12133.
Rao, D. N., Page, M. G. P., & Bickle, T. A. (1989) *J. Mol. Biol. 209*, 599–606.
Razin, A., Cedar, H., & Riggs, Eds. (1984) *DNA Methylation: Biochemistry and Biological Significance*, Springer-Verlag, New York.
Reich, N. O., & Everett, E. (1990) *J. Biol. Chem. 265*, 8929–8934.
Reich, N. O., & Mashhoon, N. (1990) *J. Biol. Chem. 265*, 8966–8970.
Reich, N. O., Maegley, K. A., Shoemaker, D. D., & Everett, E. (1991) *Biochemistry* (following paper in this issue).
Riggs, A. D., Bourgeois, S., & Cohn, M. (1970) *J. Mol. Biol. 53*, 401–417.
Rose, I. A. (1980) *Adv. Enzymol. Relat. Areas Mol. Biol. 64*, 47–59.
Rubin, R. A., & Modrich, P. (1977) *J. Biol. Chem. 252*, 7265–7272.
Segel, I. H. (1975) in *Enzyme Kinetics*, Wiley, New York.
Singer, P., & Wu, C.-W. (1987) *J. Biol. Chem. 262*, 14178–14189.
von Hippel, P. H., & Berg, O. G. (1989) *J. Biol. Chem. 264*, 675–678.
Wu, J., & Santi, D. V. (1987) *J. Biol. Chem. 262*, 4778–4786.
Zappia, V., Galletti, P., Porcelli, M., Manna, C., & Ragione, F. D. (1980) *J. Chromatogr. 189*, 399–405.

[4] The alternate pre-steady-state analysis starting with the Mtase–DNA complex is technically more difficult to perform. We are developing an appropriate assay system (Reich and Masshoon, unpublished observations).